Temperature dependency of material constitutive behaviour: a simple model

IOP Conf. Series: Materials Science and Engineering **651** (2019) 012051 doi:10.1088/1757-899X/651/1/012051

Temperature dependency of material constitutive behaviour: a simple model

E H Atzema [1,2]
[1] Tata Steel R&D, P.O. Box 10000, NL-1970 CA the Netherlands.
[2] Nonlinear Solid Mechanics, ET, University of Twente, the Netherlands

The realisation that the temperature in the stamping process plays an important and underestimated role is gaining recognition. In the ASPECT project [1] the implications of temperature on friction and material behaviour are modelled and used to design a control algorithm. Although the influence of temperature on the process is mainly via friction the change in material behaviour cannot be neglected. Tata Steel have long been advocates of dislocation physics based constitutive models and in this conference the results of the current modelling approach with temperature influence in the dynamic stress are presented [2] as well. For even higher accuracy a temperature influence on the static hardening part of the model can be taken into account [3] but those are in differential equation form and need to be continuously evaluated in the FEA algorithm which means adaptations in the source code. In this paper a simplified approach based for temperature influence on static hardening is presented that can be written in a closed form and thus be supplied as (tabular) hardening law to any desired FEA code.

1. Introduction

Automotive OEM's increase the number of models, albeit often on the same basic platform to try and market their cars to a more divers public. This means smaller production series because the individual models are aimed at smaller market segments. A German OEM mentioned 800 instead of 4000 part per run [4].

It has long been known that the starting up phase of a press run causes substandard performance [5] and the hypothesis is that this is mainly caused by the change in friction through heating up of the tool. Where [5] quotes 19 hours to settle on the final blank holder force, unpublished data from others suggest shorter time spans but still at least 200 products, equivalent to an hour of production.

These observations have prompted the ASPECT project proposal. ASPECT stands for Advanced Simulation and control of tribology in metal forming Processes for the North-West European Consumer goods and Transport sectors. The final aim of the ASPECT project is to design a feed forward process control based on temperature measurements. This control will be a model-based control, so an FE model of the stamping process will be built incorporating the temperature influence and establishing the temperature distribution over the tooling. In principle the transient nature of the starting up phase can be modelled (multiple strokes have been done but only for hot stamping [6] and for cold stamping only a single stroke [7]), but it is infeasible to simply simulate 200 press strokes to capture the warming up is infeasible. One activity in ASPECT is to find a way to accelerate the heat generation.

It is thought that the friction is by far the most sensitive parameter regarding temperature, [8] especially for sheet metal forming and in ASPECT much effort goes into measuring [9] and modelling [10] the temperature dependence of the friction. Nevertheless, the material behaviour is also felt to be changing enough with temperature to warrant special care. And in this paper a hardening model will

be treated that is physically based, but the derivation of the model to enable representation in tabular form directly useable in any FE code requires some simplifying assumptions.

2. Theoretical base

Any tensile test will suffer from temperature effects. The plastic deformation causes heating and this causes the material properties to change. The models that describe the material behaviour with increasing plastic strain (so-called hardening) often consist of a static part and a dynamic part. Where the dynamic part takes into account the strain rate, and the static part only the strain itself.

But as the temperature influences the measurement and the test changes the temperature this will have to be measured and corrected for before the results can be processed.

Most textbooks will give the strain rate dependence as a multiplicative term to the static hardening law. A very simple and widely used hardening law is the Swift or Nadai law:

$$\sigma = C \cdot \left(\varepsilon_p\right)^n \tag{1}$$

Relating the stress σ, to the strain ε_p, in an exponential function. The exponent, n, is referred to as hardening exponent and the C as hardening coefficient. With strain rate term in the same exponential form:

$$\sigma = C \cdot \left(\varepsilon_p\right)^n \cdot \left(\dot{\varepsilon}_p\right)^m \tag{2}$$

Now the exponent m indicates the strain rate dependence, but it exponent changes very strongly with strain rate, see e.g. [11], and thus cannot really be considered a materials constant when considering more than a decade of strain rate. Tata Steel has long experience with an additive term for strain rate dependency that is based on the activation energy needed for dislocation movements, original paper by Krabiell & Dahl [12], more recently is also used in [13]. Using dislocation dynamics it is firmly physically based. As one can imagine the activation energy is also depending on temperature. Now it will be clear why the strain rate effect was introduced above: it goes hand in hand with the effect of temperature. The additive stress dependent on strain rate and temperature is given by [12] as:

$$\sigma_{dyn} = \sigma_0^* \cdot \left[1 + \frac{kT}{\Delta G_0} \cdot ln\left(\frac{\dot{\varepsilon}}{\dot{\varepsilon}_0}\right)\right]^{m\prime} \tag{3}$$

With: σ_0^* = limit dynamic flow stress; k = Boltzmann constant = $8.617 \cdot 10^{-5}$ [eV/K]; ΔG_0 = maximum activation enthalpy; $\dot{\varepsilon}_0$ = limit strain rate for thermal activated movement; m' = power for the strain rate behaviour. Often ΔG_0 and $\dot{\varepsilon}_0$ will be taken from literature and σ_0^* and m' will be fitted.

At the same time the static hardening is also caused by dislocations. Deformation means the movement of dislocations but by moving they run into each other making it more difficult for the next one to move as well. This part obviously we would like to model on a solid physical base as well. This base is provided by Bergström [14] and amended by van Liempt [15]. This model is in differential equation form and strictly speaking needs to be incorporated in the FE model used to describe constitutive behaviour in simulations of actual forming tests. However, under certain assumptions [17] the set can be integrated, and a closed form solution obtained:

$$\sigma_{hard} = \Delta\sigma_m \cdot \left[\beta \cdot (\varepsilon + \varepsilon_0) + \left\{1 - e^{-\Omega \cdot (\varepsilon + \varepsilon_0)}\right\}^{n\prime}\right] \tag{4}$$

With $\Delta\sigma_m$ the saturation stress; Ω dislocation re-mobilisation parameter; ε_0 a pre-strain; β a linear term to account for stage IV hardening; n' power for strain hardening. Often ε_0, β and n' are based on literature and experience (0.005, 0.25 and 0.75 respectively) and only $\Delta\sigma_m$ and Ω are fitted.

Finally, there is a basic strength in the material before any dislocation start moving: σ_0. Combining the three mentioned terms a complete constitutive law is obtained:

$$\sigma_y(\varepsilon, \dot{\varepsilon}, T) = \sigma_0 + \sigma_{hard}(\varepsilon) + \sigma_{dyn}(\dot{\varepsilon}, T) \tag{5}$$

$$\sigma_y(\varepsilon, \dot{\varepsilon}, T) = \sigma_0 + \Delta\sigma_m \cdot \left[\beta \cdot (\varepsilon + \varepsilon_0) + \left\{1 - e^{-\Omega\cdot(\varepsilon+\varepsilon_0)}\right\}^{n'}\right] + \sigma_0^* \cdot \left[1 + \frac{kT}{\Delta G_0} \cdot ln\left(\frac{\dot{\varepsilon}}{\dot{\varepsilon}_0}\right)\right]^{m\prime} \tag{6}$$

In this formulation the temperature dependence is solely in the final term. However, in the experience of Tata steel R&D the parameters for this term are very similar for all steel grades. And at the same time response to temperature in the literature has been reported stronger than these parameters predict.

This means either the parameters are not correct, or some other parameter in equation (6) is not a constant but temperature dependent. In this work we propose to make Ω and $\Delta\sigma_m$ temperature dependent. Strictly speaking this violates the assumption they are constant that was used to obtain the integrated form (4). But we will do so nevertheless as we suppose the differences to be small for the limited range of temperatures we will look at.

Testing for strain rate influence sounds simple: just use a few different strain rates and fit the parameters of (3). However, all tensile tests will exhibit heating due to dissipation of plastic work, so some form of temperature correction is also needed. It is common practice to use "standard" parameters for this based on estimations given in [17], where also the observation was made that the parameters are similar for all low carbon steel grades. These standard parameters and their applicability to all grades are currently challenged [2]. Clearly, it is not enough to only test at room temperature if the "standard" parameters are suspect and if the static hardening part is also to be made dependent on temperature.

Tata Steel has already explored ways of incorporating temperature influence in the static work hardening [3], but this entails the full model of Bergström - van Liempt [14][15] for static hardening in differential equation form which necessitates modification of the FE code. For general use a form which is tabular is more practical as this can be used without modification of the code.

2.1. Sensitivity dynamic stress

In preparation for the test data to be produced an analysis of the parameter influence has been made. In the plots in Figure 1 the dynamic stress *(3)* is shown as a function of strain rate for three different temperatures. First, 5 MPa of random noise was added to the simulated measurement results and a fit was performed on this "realistic" test data. The fit was performed on 0.001; 0.1 & 10 s^{-1}, the rest of the points just show what happens in extrapolation.

Table 1: Results fitting dynamic stress parameters with noise

Parameter	Set value	Fitted value	Deviation
$\dot{\varepsilon}_0$ [s^{-1}]	1.00E+09	1.25E+09	25%
$\Delta G0$ [eV]	0.95	1.12	18%
m'	3.0	3.98	33%
σ_0^* [MPa]	800	941	18%

It shows the fit results may be way off the mark when there is a bit of noise on the measurements which there always is. However, the curves still look rather similar, see plot Figure 1.

Secondly, detailed analysis revealed that the 4 parameters in the strain rate sensitivity term show similar trends two by two. This means in parameter fitting some aliasing may occur. Changing $\dot{\varepsilon}_0$ upwards needs ΔG_0 to follow for similar results. Now the slope gets a little flatter, though. If we change σ_0^* up, we need to up m' as well to obtain similar results. But curvature gets a bit higher.

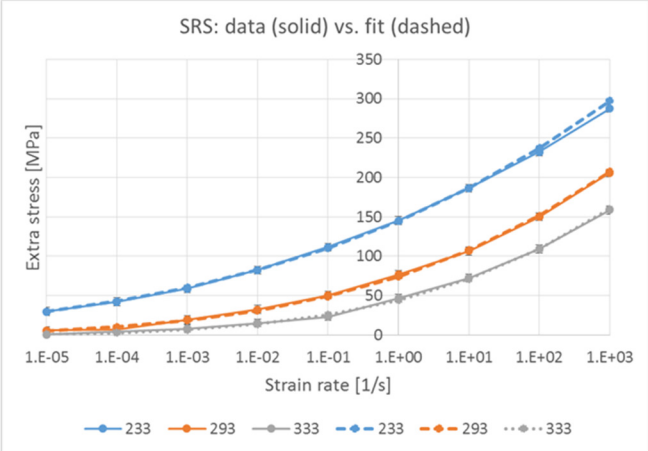

Figure 1: Fit results of dynamic stress parameters with some noise

2.2. Sensitivity static stress

Above it is stated we limit ourselves to Ω and $\Delta\sigma_m$ when looking for influence of temperature and these are the parameters normally fitted, whereas other parameters in (4) are taken from literature. The sensitivity is shown for re-mobilisation in Figure 2 basically this changes the curvature of the hardening response. The influence of the saturation stress is given in Figure 3 and this mainly changes the slope. After initial fitting of the strain rate the static hardening curves could be derived and plotted and indeed curvature and slope change slightly with temperature. These deviations in slope or curvature with temperature cannot be captured by (3) since it is additive.

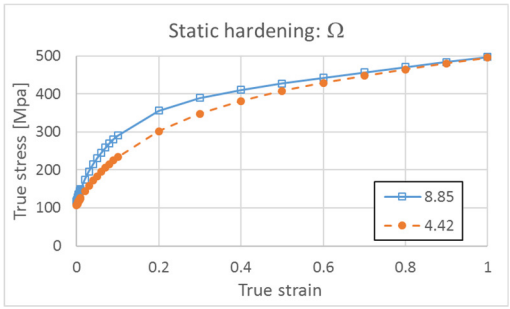

Figure 2: Influence of re-mobilisation parameter

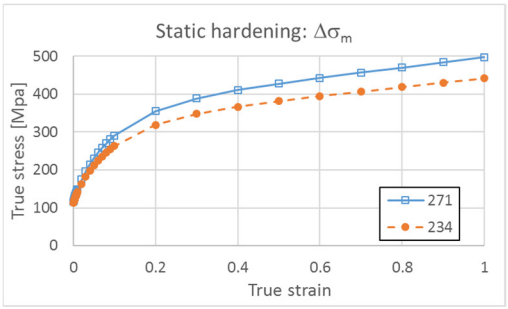

Figure 3: Influence of saturation stress

3. Practical set up

What we are looking for is the behaviour at elevated temperature, but at different strain rates since we want to apply equation (5). We choose four temperatures: 20 C, 60 C, 100 C and 140 C to cover the range of interest. The temperatures need not be kept exactly, as long as they are measured the results can be corrected accordingly. This is possible because the increase in temperature during the test is much smaller than between tests.

For strain rate three different values are used. The influence is logarithmic so a machine speeds of 1; 10 and 100 [mm/s] crosshead speeds are chosen. The latter is the practical limit of the tensile test machine, an MTS-300, so faster is not possible. The former is chosen to keep the test time acceptable, slower would not allow triplicates of all the chosen settings.

The room temperature tests (nominally 20 C) are done on the test machine as is. The elevated temperature tests are done by employing a temperature-controlled climate chamber shown in Figure 4.

Figure 4: climate chamber

It will be shown later that the increase in temperature during the test was different for the elevated temperatures than it was for room temperature tests. This can be attributed to the forced air flow which keeps the specimen closer to the environmental temperature by increasing the convection.

The temperature on the specimen was measured with a thermocouple which was clipped on, not welded on, so as not to influence the mechanical behaviour. In ASPECT multiple materials are tested but for clarity only the results of the hot dip galvanised grade, i.e. DX56D+Z. are reported here.

4. Data processing & Results

4.1. Dynamic stress

First the dynamic effect is estimated. The first two terms in (5) are the same for all strain rates and temperatures. However, some influence of strain rate and temperature on the static hardening cannot be excluded, in fact this paper aims to show a small influence is there, so the third term is best evaluated at yield stress. This excludes hardening effects, and follows procedure as seen in [16].

The lower limit for (3) is zero, it is an addition to the flow stress, cannot be a subtraction. This lower limit is referred to as the a-thermal limit, given in (7). And by plotting the Rp against the nominal strain rate the a-thermal limit of strain rate, $\dot{\varepsilon}_{ath}$, can be estimated.

$$\frac{kT}{\Delta G_0} \cdot ln\left(\frac{\dot{\varepsilon}_{ath}}{\dot{\varepsilon}_0}\right) = -1 \;\Rightarrow\; \Delta G_0 = -kT \cdot ln\left(\frac{\dot{\varepsilon}_{ath}}{\dot{\varepsilon}_0}\right) \tag{7}$$

For a single temperature the a-thermal strain rate provides a linear relationship between ΔG_0 and $\ln(\dot{\varepsilon}_0)$. For multiple temperatures these lines intersect at a unique combination of the activation energy ΔG_0 and the reference strain rate $\dot{\varepsilon}_0$.

In practice the estimation of the a-thermal strain rate at the temperatures given is not so easy because only three strain rates are available. From *Figure 5*a it was estimated that the a-thermal strain rate at 140 C is around 0.2 s^{-1}, 100 C around 0.02 s^{-1}. At 60 C and room temperature the a-thermal strain rate is cannot really be captured and lower strain rates would be needed to establish that data. For the purpose of this paper 0.002 and 0.0002 were used. Using these results for a-thermal strain rate the relationship between ΔG_0 and $\dot{\varepsilon}_0$ is plotted in *Figure 5*b. The model parameters are found by eye-balling from the graph: 1.0 [eV] for ΔG_0 and 1.0 10^9 for $\dot{\varepsilon}_0$.

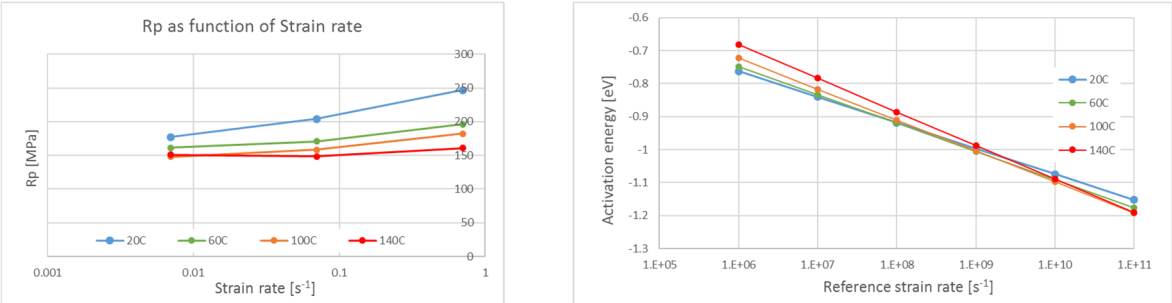

Figure 5 a: Plot of Rp against strain rate; b: determining model parameters

Now that the two basic parameters are found the σ_0^* and m' can be obtained by fitting procedures just like used in [2]. Rounded off to nice numbers 1000 MPa for σ_0^* and 1.87 for m'. This is different than the parameters mentioned in [17] (600 MPa and 2.2) but well within ranges found by [13].

4.2. Quasi-static stress

For obtaining hardening the raw test data obtained needs to be heavily processed. First the load and engineering strain are used to calculate true stress and true strain. The resolution (time wise) of the measurements is such that significant noise is seen, and for the highest speed ringing on the signal is evident. Thus the signals need to be smoothed.

After some initial attempts at moving averages a choice was made to use FFT and filter in the frequency domain. A choice prompted by the ringing frequency evident for the force signal. The strain

was filtered with a low pass at 0.4, 4 and 40 Hz for the three strain rates. The force with 5, 50 and 500 Hz. Some ringing was still apparent on the filtered force signal, but stronger filtering changed the steep initial hardening slope too much. From the smooth signals subsequently, the slope $\partial\sigma/\partial\varepsilon$ could be calculated and using a Kocks-Mecking plot both $\Delta\sigma_{\mathrm{m}}$ and Ω can be obtained for each individual test. For a description of the method see again [16]. Finally, σ_0 is used to fit all data together on the measured initial yield stress.

As all experiments were done in triplicate these values were then averaged and plotted against temperature, see Figure 6 and Figure 7. Temperature was chosen as the main axis since the over the tested range the influence of temperature is larger than strain rate.

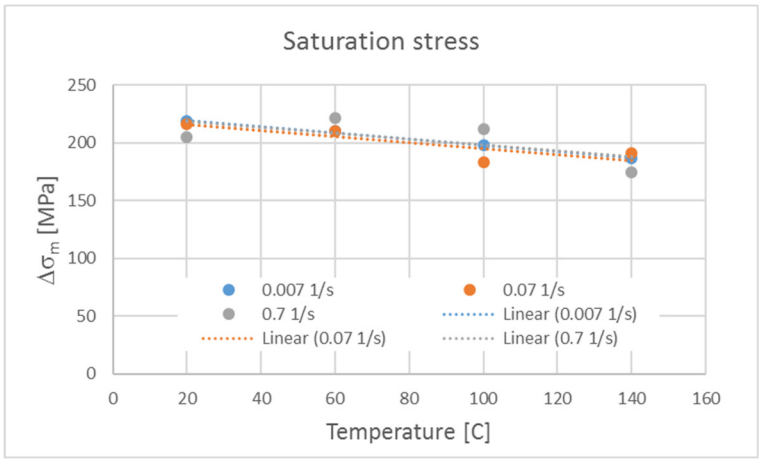

Figure 6: Fitting $\Delta\sigma_m$ against temperature for three strain rates

It would seem likely with the small deviations evident that the chosen approach could be viable. The scatter around the average would indicate that the fitting the shown trend with quadratic function is overkill and we will limit our attempt to a linear fit for both $\Delta\sigma_{\mathrm{m}}$ and Ω.

When fitting a trendline the trends in $\Delta\sigma_{\mathrm{m}}$ are nearly overlapping for all three strain rates and therefore it was concluded the influence of strain rate on $\Delta\sigma_{\mathrm{m}}$ is negligible and the influence of temperature is quantified as (8), with T in C.

$$\Delta\sigma_m = -0.26 \cdot T + 230 \tag{8}$$

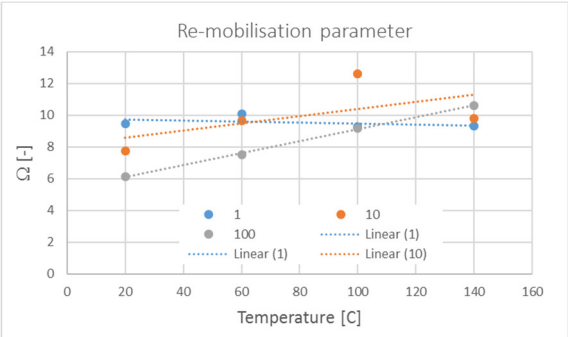

Figure 7: Fitting Ω against temperature for three strain rates

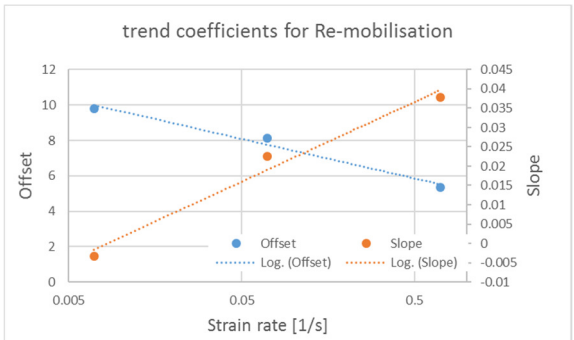

Figure 8: trend with strain rate in fit coefficients of trends in Ω with temperature

The slope and offset in linear fits of Ω against temperature seem to vary almost linear with the logarithm of the strains rate, see Figure 8. The final fit for Ω is given in (9) again with T in C.

$$\Omega = \{8.97 \cdot 10^{-3}\, ln(\dot{\varepsilon}) + 4.29 \cdot 10^{-2}\} \cdot T + \{-0.972 \ln(\dot{\varepsilon}) + 5.17\} \quad (9)$$

The processing for the static hardening parameters is based on the hardening slope $\partial\sigma/\partial\varepsilon$ and thus insensitive to strain rate. However, often the cross-head speed of a tensile test is prescribed which results in the correct nominal strain rate initially but dropping as the tensile sample elongates. For ultimate accuracy it might be advisable to correct for strain rate and then apply the procedure above. However, calculating the strain rate is a differentiating action which are notoriously sensitive to noise so additionally a moving average over a time interval of 0.2, 0.02 and 0.002 seconds respectively was still needed.

4.3. Other results

The temperature increases on the 10 mm/min cross head speed test are shown in Figure 9 for the triplicates. The blue dots are for the room temperature measurements. The other colours for elevated temperate. At elevated temperature the flow stress is lower and therefore less dissipation is expected and consequently also less increase in temperature. However, the temperature increase for the elevated temperature tests hardly differs but the difference with room temperature tests is clear. This leads us to conclude the forced air flow mitigates the temperature increase, and it is mandatory to measure the actual temperature increase to properly process the data, and not rely on the same model that is used to estimate temperature increase in normal tensile tests [17].

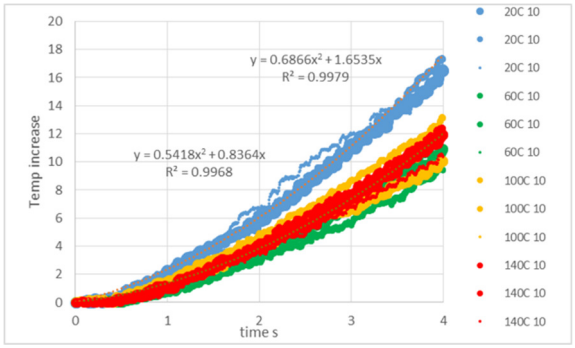

Figure 9: temperature increase

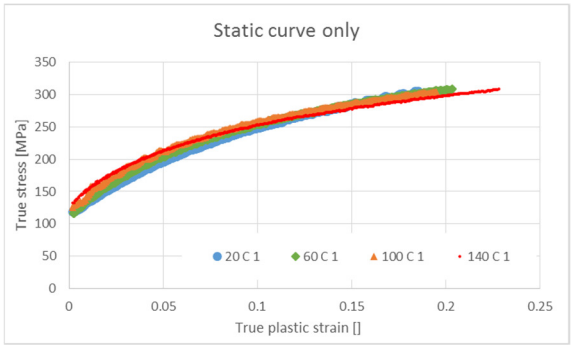

Figure 10: Example static hardening 0.007 [s^{-1}]

To show that eq (6) applies there were a few tests done with a short burst of a ten times higher strain rate as seen in [2as well. Not shown here for reasons of space, but confirming the additive nature of dynamic stress.

5. Conclusions

With the limited range in strain rates it is difficult to obtain the dynamic stress parameters accurately but the overall curves can be close nevertheless. Still it is advised to have more (at least 5) and tests lower strain rates for the lower temperatures to get a good estimate of the athermal strain rate.

For static hardening the saturation stress $\Delta\sigma_m$ was found to decrease with temperature but no significant influence of strain rate was seen. The re-mobilisation parameter Ω was found to increase with temperature and more strongly for higher strain rates.

The higher strain rates also caused ringing on the signal necessitating a lot of processing that may influence the results.

The total hardening behaviour can be captured more accurately by making the key static hardening parameters temperature dependent, whilst keeping the model so simple that it can be used in tabulated form for general use in FE independent of the code.

The use of a closed form obtained by assuming constant parameters and subsequently making these parameters vary is mathematically incorrect and the difference between the current simplification and the proper differential equations should be assessed.

Acknowledgements

This research was carried out within the project "ASPECT – Advanced Simulation and control of tribology in metal forming Processes for the North West European Consumer goods and Transport sectors", co funded by the INTERREG North West Europe programme (www.nweurope.eu/aspect.)

6. References

[1] www.nweurope.eu/aspect
[2] Abspoel M Scholting M E Lansbergen M 2019 Thermomechanical forming and crash simulations IDDRG 2019 conference
[3] Vegter H Mulder J Liempt P van Heijne J 2016 Work hardening descriptions in simulation of sheet metal forming tailored to material type and processing *Int. J. Plasticity* Volume 80 May 2016 Pages 204-221
[4] Meinhardt J 2012 *Forming in Car Body Engineering conference* Bad Nauheim 26-27 September
[5] Atzema E H 2000 PBTS3 Final report (in Dutch) Tata steel internal RefSource 104547 31-7-2000.
[6] Lorenz D Holecek M Vrolijk M Hoss M Dahmen B Doroudian M Porzner H Friberg J Koroschetz C Skrikerud M From Design Concept to Virtual Reality *Forum Stanztechnik* Bochum 2014.
[7] Fallahiarezoodar A Peker R Altan T 2016 Temperature Increase in Forming of Advanced High-Strength Steels Effect of Ram Speed Using a Servodrive Press *Journal of Manufacturing Science and Engineering* SEPTEMBER 2016, Vol. 138.
[8] Beeck J van Chezan AR Khandeparkar TV 2018 Advanced tribomechanical modelling of sheet metal forming for the automotive industry *IDDRG 2018*
[9] Filzek J 2018 ASPECT – Analyse der Reibungsveränderung durch instationäre Werkzeugtemperaturen für die Prozessauslegung und –kontrolle PtU Darnmstadt *Triboforum 2018*
[10] Wang C, Hazrati J, de Rooij M B, Veldhuis M, Aha B, Georgiou E, Drees D, Boogaard A H van den 2018 Temperature dependent micromechanics-based friction model for cold stamping processes, in *Numisheet 2018*
[11] Kovac F Dzubinsky M Boruta J 2003 Prediction of low carbon steels behaviour under hot rolling service conditions *Acta Materialia* 51 (2003) 1801–1808; Received 2 August 2002; received in revised form 20 November 2002; accepted 30 November 2002
[12] Krabiell A Dahl W 1981 Zum Einfluss von Temperatur und Dehngeschwindigkeit auf die Streckgrenze von Baustählen unterschiedlicher Festigjkeit, Arch. Eisenhüttenwesen, 52 (1981)
[13] Larour P 2010 Strain rate sensitivity of automotive sheet steels: influence of plastic strain, strain rate, temperature, microstructure, bake hardening and pre-strain PhD Thesis RWTH Aachen 22-4-2010
[14] Bergström Y 1969 A Dislocation model for the stress strain behaviour of polycrystalline a-Fe with special emphasis on the variation of the densities of mobile and immobile dislocations *Mat. Sci. Eng.* 5 (1969/1970) p 179-192
[15] Liempt P van 2016 Yield and flow stress of steel in the austenitic state PhD thesis Technical University of Delft Delft 29 11 2016
[16] Abspoel M Neelis B Liempt P van 2016 Constitutive behaviour under hot stamping conditions Journal of Materials Processing Technology 228 (2016) 34–42
[17] Vegter H On the plastic behaviour of steel during sheet forming PhD thesis University of Twente Enschede 4-10-1991